**EUROPEAN JOURNAL OF PURE AND APPLIED MATHEMATICS**
2025, Vol. 18, Issue 3, Article Number 5970
ISSN 1307-5543 – ejpam.com
Published by New York Business Global

# Spatio-Temporal Graph Neural Network for Time Series Forecasting: Local Antimagic Coloring-Based Companion Farming

A. I. Kristiana[1,2], R. Izza[3], I. H. Agustin[1,4,*], L. A. Monalisa[2], I. L. Mursyidah[1], R. I. Baihaki[1], K. H. Agustina[5], Dafik[1,4]

[1] *PUI-PT Combinatorics and Graph, CGANT, University of Jember, Jember, Indonesia*
[2] *Department of Mathematics Education, University of Jember, Jember, Indonesia*
[3] *Department of Mathematics Education, Cordoba Islamic University, Banyuwangi, Indonesia*
[4] *Department of Mathematics, University of Jember, Jember Indonesia*
[5] *Department of Postgraduate Mathematics Education , University of Jember, Jember, Indonesia*

**Abstract.** Let $G(V, E)$ represent a simple, finite, and connected graph with $|V| = p$ and $|E| = q$. A bijection $f : V(G) \longrightarrow \{1, 2, 3, \ldots, |V(G)|\}$ is defined as an edge antimagic labeling of $G$ if the edge weights $w(uv) = f(u) + f(v)$, where $uv \in E(G)$, are all distinct. This labeling induces a lea coloring of $G$, where each edge is assigned a color based on its weight $w(e)$. The graph $G$ is said to have a local $(a, d)$-edge antimagic coloring if the edge colors form an arithmetic sequence with an initial term $a$ and a common difference $d$. The edge weights then belong to an arithmetic progression $\{a, a + d, a + 2d, \ldots, a + (k - 1)d\}$, where $a, d \geq 1$ are integers, and $k$ represents the number of distinct colors used. The minimum number of colors required for $G$ to admit a local $(a, d)$-edge antimagic coloring is called the local $(a, d)$-edge antimagic chromatic number, denoted by $\chi_{le(a,d)}(G)$. This coloring is referred to as lea$(a, d)$ coloring. In this study, we establish both the lower and upper bounds of $\chi_{le(a,d)}(G)$ and identify the exact values for specific graph classes. Additionally, we demonstrate the practical application of local $(a, d)$-edge antimagic coloring by employing it in the analysis of the Spatio-Temporal Graph Neural Network (STGNN) model to support autonomous Controlled Environment Agriculture (CEA) in forecasting NPK concentration trends for companion plantations over multiple time steps.

**2020 Mathematics Subject Classifications**: 05C15, 05C90, 68R01, 68R10

**Key Words and Phrases**: Local $(a, d)$-edge antimagic coloring, Spatio-Temporal Graph Neural Network (STGNN), NPK concentration forecasting

*Corresponding author.
DOI: https://doi.org/10.29020/nybg.ejpam.v18i3.5970

*Email addresses:* ikahesti.fmipa@unej.ac.id (I. H. Agustin)

 

## 1. Introduction

In addition, a local edge antimagic coloring can also be defined for graphs [1]. A bijection $f : V \to \{1, 2, 3, \ldots, |V(G)|\}$ is referred to as a *lea labeling* if any two adjacent edges $e_1$ and $e_2$ satisfy $w(e_1) \neq w(e_2)$, where for $e = uv \in E(G)$, the weight of the edge is given by $w(e) = f(u) + f(v)$. A proper edge coloring of $G$ is induced by the lea labeling when all edges are assigned colors based on their weights $w(e)$ [2]. The *lea chromatic number*, represented as $\chi_{lea}(G)$, denotes the minimum number of colors required for the proper edge coloring of $G$ based on the lea labeling [3]. Several findings related to lea coloring in graphs are discussed in [4]. A graph $G$ is said to have a *local* $(a, d)$*-antimagic coloring* if the set of its edge colors forms an arithmetic progression $\{a, a+d, a+2d, \ldots, a+(k-1)d\}$, where $a, d \geq 1$ are integers, and $k$ is the number of distinct colors used in the proper edge coloring. This type of coloring is referred to as a *lea*$(a, d)$ *coloring*. The *local* $(a, d)$*-antimagic chromatic number*, denoted as $\chi_{le(a,d)}(G)$, is defined as the minimum number of colors required to assign a local $(a, d)$-antimagic coloring to $G$. For further details, refer to [5].

The study of graph colorings has been an essential area of research in combinatorics, particularly due to its wide-ranging applications in network optimization, scheduling, and cryptographic systems [6, 7]. Several recent works have contributed significantly to advancing this field. For example, Alfarisi et al. explored the graceful chromatic number of unicyclic graphs, establishing critical properties and applications in network models [8]. Similarly, Dafik et al. examined the non-isolated resolving numbers of special graphs, offering insights into their operational characteristics and implications for graph operations [9]. Building on these foundations, Septyory et al. (2021) focused on rainbow antimagic coloring of special graphs, showcasing its potential in diverse computational frameworks [10]. Further, Dafik et al. and Gembong et al. investigated edge domination numbers and distance domination numbers in comb product graphs, respectively, providing a deeper understanding of their structural and combinatorial properties [11].

As a subfield of graph coloring, local edge-antimagic $(a, d)$-coloring (lea$(a, d)$ coloring) has been the subject of numerous studies. Rajkumar and Nalliah [12] computed the lea$(a, d)$-chromatic number for wheel graphs. Agustin et al. (2023) further analyzed path, fan, friendship, and star graphs to determine their respective lea$(a, d)$-chromatic numbers [13]. Almaidah et al. (2023) studied ladder, cycle, octopus, helm, triangular book, and tadpole graphs [14]. Putra et al. extended the analysis to centipede, lotus, caterpillar, double star, and double broom graphs [15]. Rifda et al. (2023) explored the application of lea$(a, d)$ coloring on broom, book, firecracker, complete, and dragon graphs [16].

Despite the significant progress made in the study of lea$(a, d)$ coloring across various graph classes, its application to real-world domains remains limited. To the best of our knowledge, no prior work has integrated the concept of lea$(a, d)$ coloring into smart agriculture, particularly within the framework of Spatio-Temporal Graph Neural Networks (STGNN). This research addresses that gap by proposing a novel integration of graph labeling theory and deep learning for optimized sensor deployment and nutrient forecasting.

Recent developments further support the feasibility of incorporating graph coloring

concepts into deep learning models for agricultural forecasting. Expanding the application of graph coloring, Kristiana et al. (2024) analyzed the b-coloring of graphs and its integration into Spatio-Temporal Graph Neural Networks (STGNN) for multi-step time series forecasting [17]. Their study demonstrated how graph coloring techniques could optimize the monitoring of soil moisture and pH levels in companion farming systems [18]. These findings reinforce the significance of graph coloring not only in theoretical combinatorial problems but also in practical applications, particularly in agricultural and environmental monitoring [19]. Collectively, these studies highlight the growing importance of graph coloring techniques in addressing both theoretical challenges and real-world problems in combinatorics and beyond [20].

This research is motivated by the need to bridge the gap between theoretical developments in graph labeling and their practical applications in data-driven systems. Specifically, this paper aims to derive sharper lower and upper bounds for the lea$(a,d)$-chromatic number, $\chi_{le(a,d)}(G)$, and to determine its exact value for selected classes of graphs. Beyond the theoretical contributions, this study demonstrates the applicability of lea$(a,d)$ coloring in real-world scenarios by integrating it into the analysis of a STGNN model. This integration is applied in the context of autonomous Controlled Environment Agriculture (CEA), where it supports multi-step time series forecasting of nitrogen (N), phosphorus (P), and potassium (K) concentrations in companion plantation systems. The proposed approach not only advances graph coloring theory but also enhances predictive accuracy and sensor efficiency in precision agriculture.

## 2. Method

This research utilizes both analytical and experimental methodologies. In the analytical section, we will apply a mathematical deductive approach to obtain some theorems, we use the the following some known lower bounds to obtain the new theorems.

**Observation 1.** *[1]* $\chi_{lea}(G) \geq \chi(G)$*, where* $\chi(G)$ *is a chromatic number of graph coloring* $G$*.*

**Observation 2.** *[3]* $\chi_{le(a,d)}(G) \geq \chi_{lea}(G) \geq \chi(G)$

**Observation 3.** *[1]* $\chi_{lea}(G) \geq \Delta(G)$*, where* $\Delta(G)$ *is maximum degrees of* $G$

**Observation 4.** *[13]* $\chi_{le(a,d)}(G) \geq \chi_{lea}(G) \geq \Delta(G)$

**Observation 5.** *[16]* $\chi_{le(a,d)}(G) \geq \chi_{lea}(G) \geq \chi(G) \geq \Delta(G)$*.*

**Observation 6.** *[16] If the graph* $G$ *admits an local* $(a,d)$*-edge antimagic labeling with* $k$*-colors, then* $d \leq \frac{2p-4}{k-1}$*.*

Whilst, in the experimental method, we will use a computer programming to do simulation on autonomous Controlled Environment Agriculture (CEA) development on multi-step time series forecasting for NPK concentration of companion plantations of Rosa *sp.*

plantation, Bougainvillea spectabilis plantation, Cryptanthus spp plantation, and Bromeliaceae plantation. First, we will display the vertex embedding process of a single-layer GNN for a given graph that contains three feature data, namely N, P, and K data for three month observation. Second, we will write STGNN programming, train a model utilizing 80% of the input data obtained from the vertex embedding process, test and finally forecast the NPK fertilization to determine the time of application of fertilizer to Rosa sp plantation, Bromeliaceae plantation, Bougainvillea spectabilis plantation and Cryptanthus sp plantation. We use the Algorithm 1 for studying the fuel purchase distribution by using STGNN combined by lea$(a, d)$ coloring.

**Algorithm 1** (phtb)**.** *InputInput OutputOutput*

*Graph $G(V, E)$, adjacency matrix $A$ from graph $G$, feature matrix $H_{n\times m}$, and threshold $\epsilon$ Time series prediction results*

*Initialize parameters: weights $W$, bias $\beta$, and learning rate $\alpha$.*

*error $< \epsilon$ Perform message propagation $\mathbf{m_u}^{\lambda} = MSG_{\lambda}(h_u^{\lambda-1})$.*
*Compute aggregated message $h_v^{\lambda} = AGG_{\lambda}\{m_u^{\lambda-1},\ u \in N(v)\}$.*
*Evaluate error $\lambda = \frac{||h_{v_i} - h_{v_j}||_2}{|E|}$.*
*Update parameters: $W_j^{\lambda+1} = W_j^{\lambda} + \alpha \cdot z_j \cdot e^{\lambda}$.*

*Store the final node representations as embedding vector.*
*Load the feature embedding from saved data.*
*Apply forecasting using learned representations.*
*Output the best-fit prediction based on training and validation.*

*Single-Layer Graph Neural Network for Forecasting*

## 3. Main Result

### 3.1. Local $(a, d)$-edge Antimagic Coloring

In this section, we will show the existence of lea$(a, d)$ coloring of a some specific families of graphs, and determine the exact value of the lea$(a, d)$ chromatic number of $P_n \triangleright P_m$, $amal(F_n, v, m)$, and $amal(\mathcal{V}_n, v, m)$. Further, we will use the obtained theorem for analysing STGNN model for autonomous Controlled Environment Agriculture (CEA) development on multi-step time series forecasting for NPK concentration of companion plantations.

**Theorem 1.** *Let $P_n \triangleright P_m$ be a comb product between $P_n$ and $P_m$ graph with $n, m \geq 3$. We have $\chi_{le(nm-n+3,2)}(P_n \triangleright P_m) = n$, for $m \equiv 1(mod\ 2)$, $n \equiv 0(mod\ 2)$; and $\chi_{le(nm+1,2)}(P_n \triangleright P_m) = n$, for $m, n \equiv 0(mod\ 2)$.*

*Proof.* We begin by recalling the structure of the comb product $P_n \triangleright P_m$, which is a connected graph composed of $n$ copies of the path $P_m$, where each $P_m$ is connected via its

last vertex to form a path of $n$ vertices. Formally, the vertex set is given by $V(P_n \triangleright P_m) = \{x_j^i : 1 \leq i \leq n, 1 \leq j \leq m\}$ and the edge set is defined as $E(P_n \triangleright P_m) = \{x_j^i x_{j+1}^i : 1 \leq j \leq m-1, 1 \leq i \leq n\} \cup \{x_m^i x_m^{i+1} : 1 \leq i \leq n-1\}$. Consequently, we have $|V| = nm$ and $|E| = nm - 1$.

To prove the theorem, we determine both the lower and upper bounds of the local edge $(a, d)$-antimagic chromatic number and show that they are equal to $n$ under the given conditions.

From the result by Agustin et al. [2], it is known that $\chi_{lea}(P_n \triangleright P_m) = n$ for $n, m \geq 3$. Additionally, Observation 2 implies $\chi_{le(a,d)}(P_n \triangleright P_m) \geq \chi_{lea}(P_n \triangleright P_m) = n$. Thus, the lower bound is established.

To construct the upper bound, we define a bijective labeling $f : V(P_n \triangleright P_m) \to \{1, 2, \ldots, nm\}$ as follows:

$$f(x_j^i) = \begin{cases} i + \frac{(j-1)n}{2}, & \text{if } j \equiv 1 \pmod 2 \\ nm + 1 - i + n - \frac{nj}{2}, & \text{if } j \equiv 0 \pmod 2 \end{cases}$$

This labeling ensures a proper assignment of distinct values to the vertices and generates edge weights that can be analyzed in two separate cases based on the parity of $m$ and $n$.

**Case 1:** For $m \equiv 1 \pmod 2$ and $n \equiv 0 \pmod 2$, the edge weights for horizontal edges within each copy of $P_m$ are:

$$w(x_j^i x_{j+1}^i) = \begin{cases} nm + 1, & \text{if } j \equiv 1 \pmod 2 \\ nm + n + 1, & \text{if } j \equiv 0 \pmod 2 \end{cases}$$

For vertical edges between copies:

$$w(x_m^i x_m^{i+1}) = nm - n + 2i + 1, \quad \text{for } 1 \leq i \leq n-1$$

These edge weights can be grouped into three distinct sets: $W_1 = \{nm + 1\}$, $W_2 = \{nm + n + 1\}$, and $W_3 = \{nm - n + 3, nm - n + 5, \ldots, nm + n - 1\}$. We examine their cardinalities and mutual disjointness.

To verify disjointness: suppose $W_1 \subseteq W_3$ implies $nm + 1 = nm - n + 2i + 1$, which leads to $i = \frac{n}{2}$. Since $i = \frac{n}{2}$ is within the index range, it confirms $W_1 \subset W_3$. On the other hand, suppose $W_2 \subseteq W_3$ implies $nm + n + 1 = nm - n + 2i + 1$, which leads to $i = n$. However, $i = n$ lies outside the valid range of $1 \leq i \leq n - 1$, hence a contradiction. Therefore, $W_2 \cap W_3 = \emptyset$ and $W = W_2 \cup W_3$.

The cardinality is then $|W_2| = 1$, and for $W_3$, let $U_s$ be the $s$-th term in the arithmetic progression with common difference 2. Solving $nm + n - 1 = nm - n + 3 + (|W_3| - 1) \cdot 2$, we find $|W_3| = n - 1$, so $|W| = n$.

**Case 2:** For $m, n \equiv 0 \pmod 2$, we compute:

$$w(x_m^i x_m^{i+1}) = nm + 2n - 2i + 1, \quad \text{for } 1 \leq i \leq n-1$$

The weight sets in this case are $W_1 = \{nm+1\}$, $W_2 = \{nm+n+1\}$, and $W_3 = \{nm+2n-1, nm+2n-3, \ldots, nm+3\}$.

To verify disjointness: suppose $W_1 \subseteq W_3$ implies $nm+1 = nm+2n-2i+1$, which gives $i = n$. Since $i = n$ is out of range, this leads to a contradiction. Hence $W_1 \cap W_3 = \emptyset$. Now suppose $W_2 \subseteq W_3$ implies $nm+n+1 = nm+2n-2i+1$, which gives $i = \frac{n}{2}$. Since this $i$ lies within the valid range, $W_2 \subset W_3$, and thus $W = W_1 \cup W_3$.

The cardinality is $|W_1| = 1$. To compute $|W_3|$, let $U_s = nm+3$ and $U_1 = nm+2n-1$. Solving $U_s = U_1 + (s-1)(-2)$, we obtain $s = n-1$, so again $|W| = n$.

Therefore, in both cases, we have $\chi_{le(a,d)}(P_n \triangleright P_m) \leq n$ and from the lower bound, equality holds. Hence the theorem is proved. □

**Theorem 2.** *Let $amal(F_n, x, m)$ be an amalgamation of fan graph with $n \geq 3$ and $m \geq 2$. We have $nm \leq \chi_{le(nm+1,1)}(amal(F_n, x, m)) \leq nm+1$.*

*Proof.* Amalgamation of fan graph $amal(F_n, x, m)$ is a connected graph with vertex set $V(amal(F_n, x, m)) = \{x\} \cup \{x_i^j; 1 \leq i \leq n, 1 \leq j \leq m\}$ and edge set $E(amal(F_n, v, m)) = \{xx_i^j; 1 \leq i \leq n, 1 \leq j \leq m\} \cup \{x_i^j x_{i+1}^j; 1 \leq i \leq n-1, 1 \leq j \leq m\}$. The cardinality of the vertices set $|V(amal(F_n, x, m))| = nm+1$, and the cardinality of the edges set $|E(amal(F_n, x, m))| = 2nm - m$.

To prove, first we need to show the lower bound of $\chi_{le(nm+1,1)}(amal(F_n, x, m))$. Based on Observation 4, we have $\chi_{le(a,d)}(amal(F_n, x, m)) \geq \chi_{lea}(amal(F_n, x, m)) \geq \Delta(amal(F_n, x, m))$. The maximum degree is $\Delta(amal(F_n, x, m)) = nm$. Thus, the lower bound is $\chi_{le(a,d)}(amal(F_n, x, m)) \geq nm$. To show the upper bound, we define the bijection as follow $f : V(amal(F_n, x, m)) \to \{1, 2, 3, \ldots, |V(amal(F_n, x, m))|\}$. To prove upperbound, we show into two cases.

**Case 1.** For $n \equiv 1(mod 2)$, we have the following.
Firstly, we show the bijective function of vertex labels as follows

$$f(x) = nm+1$$

$$f(x_i^j) = \begin{cases} \frac{nj+n+i+1}{2} - n, & for\ i,j \equiv 1(mod\ 2) \\ nm - \frac{nj+n+i}{2} + n + 1, & for\ i \equiv 1(mod\ 2),\ j \equiv 0(mod\ 2) \\ \frac{nj+n+i+1}{2} - n, & for\ i,j \equiv 0(mod\ 2) \\ nm - \frac{nj+n+i}{2} + n + 1, & for\ i \equiv 0(mod\ 2),\ j \equiv 1(mod\ 2) \end{cases}$$

Under the bijection $f$, the edge weights can be presented as follows

$$w(x_i^j x_{i+1}^j) = \begin{cases} nm+1, & for\ m,i \equiv 1(mod\ 2) \\ nm+2, & for\ m \equiv 1(mod\ 2),\ i \equiv 0(mod\ 2) \\ nm+1, & for\ m,i \equiv 0(mod\ 2) \\ nm+2, & for\ m \equiv 0(mod\ 2),\ i \equiv 1(mod\ 2) \end{cases}$$

$$w(xx_i^j) =$$

$$\begin{cases} \frac{nj+n+i+1}{2} - n + nm + 1, & for\ i,j \equiv 1(mod\ 2),\ 1 \leq i \leq n, 1 \leq j \leq m \\ 2nm - \frac{jn+n+i}{2} + n + 2, & for\ i \equiv 1(mod\ 2),\ j \equiv 0(mod\ 2),\ 1 \leq i \leq n, 2 \leq j \leq m \\ \frac{nj+n+i+1}{2} - n + nm + 1, & for\ i,j \equiv 0(mod\ 2),\ 2 \leq i \leq n, 2 \leq j \leq m \\ 2nm - \frac{jn+n+i}{2} + n + 2, & for\ i \equiv 0(mod\ 2),\ j \equiv 1(mod\ 2),\ 2 \leq i \leq n, 1 \leq j \leq m \end{cases}$$

Thus, we can write in the form of the set W of edge weight of $amal(F_n, x, m)$. It includes four sets of edge weights, namely $W_1 = \{nm+1\}$, $W_2 = \{nm+2\}$, $W_3 = \{nm+2, nm+3, nm+4 \ldots, nm+1+\frac{nm+1}{2}\}$, and $W_4 = \{nm+2+\frac{nm+1}{2}, nm+3+\frac{nm+1}{2}, \ldots, 2nm+1\}$. Our task is to determine the cardinality of those sets to obtain the upper bound, but we need to check whether all three sets are disjoint or not first. Under the contradiction proof, we suppose $W_1 \subseteq W_3 \longleftrightarrow nm+1 = \frac{nj+n+i+1}{2} - n + nm + 1 \longleftrightarrow i = -3n - nj - 1$. Since $w(xx_i^j) = \frac{nj+n+i+1}{2} - n + nm + 1$, for $1 \leq i \leq \frac{nm+1}{2}$, therefore $i = -3n - nj - 1$ does not lie in the interval, it is a contradiction. We conclude that $W_1 \cap W_3 = \varnothing$. Furthermore, in the contradiction proof, we suppose $W_1 \subseteq W_4 \longleftrightarrow nm+1 = 2nm - \frac{nj+n+i}{2} + n + 2 \longleftrightarrow i = 2nm - nj + 2$. Since $w(xx_i^j) = 2nm - \frac{nj+n+i}{2} + n + 2$, for $\frac{nm+3}{2} \leq i \leq nm$, therefore $i = 2nm - nj + 2$ does not lie in the interval, it is a contradiction. We conclude that $W_1 \cap W_4 = \varnothing$. Finally, we have $W = W_1 \cup W_3 \cup W_4$.

Now, we can determine the cardinality of W. First, it is easy to see that $|W_1| = 1$, secondly we will determine $|W_3 \cup W_4|$, under the following calculation. Let $U_s$ and $d$ be the $s$ term and different from the arithmetic sequence of $W_3 \cup W_4$, consequently. We have $U_{|W_3 \cup W_4|} = a + (|W_3 \cup W_4| - 1)d \longleftrightarrow 2nm+1 = nm+2+(|W_3 \cup W_4|-1)1 \longleftrightarrow |W_3 \cup W_4| = nm$. $W_3 \cup W_4$ form an arithmetic sequence with initial value $a = nm+2$ and $W_2 = nm+2$. Thus, we have $W_2 \subset (W_3 \cup W_4)$. This implies $|W| = |W_1| + |W_3 \cup W_4| = 1 + nm$. Finally, we have $\chi_{le(nm+1,1)}(amal(F_n, x, m)) \leq nm + 1 \quad for\ n \equiv 1(mod\ 2)$.

**Case 2.** For $n \equiv 0(mod 2)$, we have the following.
Firstly, we show the bijective function of vertex labels as follows.

$$f(x) = nm + 1$$

$$f(x_i^j) = \begin{cases} \frac{nj-n+i+1}{2}, & for\ i \equiv 1(mod\ 2), 1 \leq i \leq n, 1 \leq j \leq m \\ nm - \frac{i+nj-n}{2} + 1, & for\ i \equiv 0(mod\ 2), 2 \leq i \leq n, 1 \leq j \leq m \end{cases}$$

Under bijection $f$, the edge weights can be presented as follows.

$$w(x_i^j x_{i+1}^j) = \begin{cases} nm+1, & for\ i \equiv 1(mod\ 2), 1 \leq i \leq n-1, 1 \leq j \leq m \\ nm+2, & for\ i \equiv 0(mod\ 2), 2 \leq i \leq n-1, 1 \leq j \leq m \end{cases}$$

$$w(xx_i^j) = \begin{cases} nm+1+\frac{nj-n+i+1}{2}, & for\ i \equiv 1(mod\ 2),\ 1 \leq i \leq n, 1 \leq j \leq m \\ 2nm+2-\frac{i+nj-n}{2}, & for\ i \equiv 0(mod\ 2),\ 2 \leq i \leq n, 1 \leq j \leq m \end{cases}$$

Thus, we can write in the form of the set W of edge weight of $amal(F_n, x, m)$. It includes four sets of edge weights, namely $W_1 = \{nm+1\}$, $W_2 = \{nm+2\}$, $W_3 = \{nm+2, nm+3, nm+4, \ldots, nm+1+\frac{nm}{2}\}$, and $W_4 = \{nm+2+\frac{nm}{2}, nm+3+\frac{nm}{2}, nm+4+\frac{nm}{2} \ldots, 2nm+1\}$. Our task is to determine the cardinality of those sets to obtain the upper bound, but we need to check whether all three sets are disjoint or not first. Under the contradiction proof, we suppose $W_1 \subseteq W_3 \longleftrightarrow nm+1 = nm+1+\frac{nj-n+i+1}{2} \longleftrightarrow i = n - nj - 1$. Since $w(xx_i^j) = nm + 1 + \frac{nj-n+i+1}{2}$, for $1 \leq i \leq \frac{nm}{2}$, therefore $i = n - nj - 1$ does not lie in the interval, it is a contradiction. We conclude that $W_1 \cap W_3 = \varnothing$. Furthermore, in the contradiction proof, we suppose $W_1 \subseteq W_4 \longleftrightarrow nm+1 = 2nm+3-\frac{i+nj-n}{2} \longleftrightarrow$

$i = 2nm - nj + n + 4$. Since $w(xx_i^j) = 2nm + 3 - \frac{i+nj-n}{2}$, for $\frac{nm+1}{2} \leq i \leq nm$, therefore $i = 2nm - nj + n + 4$ does not lie in the interval, it is a contradiction. We conclude that $W_1 \cap W_4 = \varnothing$. Finally, we have $W = W_1 \cup W_3 \cup W_4$.

Now, we can determine the cardinality of W. First, it is easy to see that $|W_1| = 1$, secondly we will determine $|W_3 \cup W_4|$, under the following calculation. Let $U_s$ and $d$ be the $s$ term and different from the arithmetic sequence of $W_3 \cup W_4$, consequently. We have $U_{|W_3 \cup W_4|} = a+(|W_3 \cup W_4|-1)d \longleftrightarrow 2nm+1 = nm+2+(|W_3 \cup W_4|-1)1 \longleftrightarrow |W_3 \cup W_4| = nm$. $W_3 \cup W_4$ form an arithmetic sequence with initial value $a = nm+2$ and $W_2 = nm+2$ then we have $W_2 \subset (W_3 \cup W_4)$. It implies that $|W| = |W_1| + |W_3 \cup W_4| = 1 + nm$. Finally, we have $\chi_{le(nm+1,1)}(amal(F_n, x, m)) \leq nm + 1 \quad for\ n \equiv 1(mod\ 2)$.

Thus, we will have $\chi_{le(nm+1,1)}(amal(F_n, x, m)) \leq nm + 1$. It can be concluded that $nm \leq \chi_{le(nm+1,1)}(amal(F_n, x, m)) \leq nm + 1$.

**Theorem 3.** *Let $amal(\mathcal{V}_n, x, m)$ be an amalgamation of volcano graph with $n, m \geq 2$. We have $\chi_{le(3,1)}(amal(\mathcal{V}_n, x, m)) = 2m + nm$.*

*Proof.* Amalgamation of volcano graph $amal(\mathcal{V}_n, x, m)$ is a connected graph with vertex set $V(amal(\mathcal{V}_n, x, m)) = \{x\} \cup \{x_i; 1 \leq i \leq m\} \cup \{z_i; 1 \leq i \leq m\} \cup \{y_i; 1 \leq i \leq nm\}$ and edge set $E(amal(\mathcal{V}_n, x, m)) = \{x_i z_i; 1 \leq i \leq m\} \cup \{xx_i; 1 \leq i \leq m\} \cup \{xz_i; 1 \leq i \leq m\} \cup \{xy_i; 1 \leq i \leq nm\}$. The cardinality of the vertices set $|V(amal(\mathcal{V}_n, x, m))| = nm+2m+1$, and the cardinality of the edges set $|E(amal(\mathcal{V}_n, x, m))| = nm + 3m$.

To prove this theorem, first, we need to show the lower bound of $\chi_{le(3,1)}(amal(\mathcal{V}_n, x, m))$. Agustin et al in [1] If $\Delta(G)$ is maximum degrees of $G$ then we have the local edge antimagic chromatic number of $\chi_{lea}(G) \geq \Delta(G)$. Based on Observation 3 we have $\chi_{le(a,d)}(amal(\mathcal{V}_n, x, m)) \geq \chi_{lea}(amal(\mathcal{V}_n, x, m)) \geq \Delta(amal(\mathcal{V}_n, x, m))$. $\Delta(amal(\mathcal{V}_n, x, m))$ is $2m + nm$. Thus, the lower bound is $\chi_{le(a,d)}(amal(\mathcal{V}_n, x, m)) \geq 2m + nm$. To show the upper bound, we define the bijection as follow $f : V(amal(\mathcal{V}_n, x, m)) \to \{1, 2, 3, \ldots, |V(amal(\mathcal{V}_n, x, m))|\}$.

$$f(x) = 1$$

$$f(x_i) = i + 1, for\ 1 \leq i \leq m$$

$$f(y_i) = 2m + i + 1, for\ 1 \leq i \leq nm$$

$$f(z_i) = 2m - i + 2, for\ 1 \leq i \leq m$$

Under the bijection $f$, the edge weights can be presented as follows

$$w(xx_i) = i + 2, for\ 1 \leq i \leq m$$

$$w(x_i z_i) = 2m + 3, for\ 1 \leq i \leq m$$

$$w(xz_i) = 2m - i + 3, for\ 1 \leq i \leq m$$

$$w(xy_i) = 2m + 2 + i, for\ 1 \leq i \leq mn$$

Thus we can write in the form of set $W$ of edge weight of $amal(\mathcal{V}_n, x, m)$. It includes three edge weight sets, namely $W_1 = \{3, 5, \cdots, 2 + m\}, W_2 = \{2m + 3\}$, $W_3 = \{2m + 2, 2m + 1 \cdots, m + 3\}$, and $W_4 = \{2m + 3, 2m + 4, \cdots, 2m + 2 + n\}$. Our task is to determine the cardinality of those sets to obtain the upper bound, but we need to check weather all three sets are disjoint or not first. Under the contradiction proof, we suppose $W_2 \subseteq W_1 \longleftrightarrow 2m + 3 = 2 + i \longleftrightarrow i = 2m + 1$. Since $w(xx_i) = 2 + i$, for $1 \leq i \leq m$, thus $i = 2m+1$ does not lie in the interval, it is a contradiction. It concludes that $W_2 \cap W_1 = \varnothing$. Under the contradiction proof, we suppose $W_1 \subseteq W_3 \longleftrightarrow 2+i = 2m-i+3 \longleftrightarrow i = \frac{2m+1}{2}$. Since $w(xz_i) = 2m - i + 3$, for $1 \leq i \leq m$, thus $i = \frac{2m+1}{2}$ does not lie in the interval, it is a contradiction. It concludes that $W_1 \cap W_3 = \varnothing$.Under the contradiction proof, we suppose $W_1 \subseteq W_4 \longleftrightarrow 2 + i = 2m + 2 + i \longleftrightarrow m = 0$. Since $w(xy_i) = 2m + 2 + i$, for $1 \leq i \leq mn$, thus $m = 0$ does not lie in the interval, it is a contradiction. It concludes that $W_1 \cap W_4 = \varnothing$. Under the contradiction proof, we suppose $W_2 \subseteq W_3 \longleftrightarrow 2m + 3 = 2m - i + 3 \longleftrightarrow i = 0$. Since $w(xz_i) = 2m - i + 3$, for $1 \leq i \leq m$, thus $i = 0$ does not lie in the interval, it is a contradiction. It concludes that $W_2 \cap W_3 = \varnothing$. Under the contradiction proof, we suppose $W_2 \subseteq W_4 \longleftrightarrow 2nm+3 = 2m+2+i \longleftrightarrow i = 1$. Since $w(xy_i) = 2m+2+i$, for $1 \leq i \leq mn$, thus $i = 1$ lies in the interval. It concludes that $W_2 \subset W_4$. Furthermore, under the contradiction proof, we suppose $W_3 \subseteq W_4 \longleftrightarrow 2nm - 1 + 3 = 2m + 2 + i \longleftrightarrow i = \frac{1}{2}$. Since $w(xy_i) = 2m + 2 + i$, for $1 \leq i \leq mn$, thus $i = \frac{1}{2}$ does not lie in the interval, it is a contradiction. It concludes that $W_3 \cap W_4 = \varnothing$. Finally, we have $W = W_1 \cup W_3 \cup W_4$.

Now, we can determine the cardinality of $W$. First, it is easy to see that $W_2 \subset W_4$, secondly we will determine $|W_1|$, $|W_3|$ and $|W_4|$ under the following calculation. Let $U_s$ and $d$ be the $s$-term and the different of arithmetic sequence of $W_1$, $W_2$ and $W_3$, consequently. We have $U_{|W_1|} = a + (|W_1| - 1)d \longleftrightarrow 2 + m = 3 + (|W_1| - 1)1 \longleftrightarrow |W_1| = m$, $U_{|W_3|} = a+(|W_3|-1)d \longleftrightarrow m+3 = 2m+2+(|W_3|-1)(-1) \longleftrightarrow |W_3| = m$, and $U_{|W_4|} = a+(|W_4|-1)d \longleftrightarrow nm+2m+2 = 2m+3+(|W_4|-1)1 \longleftrightarrow |W_4| = nm$. It implies that $|W| = |W_1|+|W_3|+|W_4| = m+m+nm = 2m+nm$. Finally, we have $\chi_{le(3,1)}(amal(\mathcal{V}_n, x, m)) \leq 2m+nm$. Based on the lower and upper bounds, we have $2m + nm \leq \chi_{le(3,1)}(amal(\mathcal{V}_n, x, m)) \leq 2m + nm$. It can be concluded that $\chi_{le(3,1)}(amal(\mathcal{V}_n, x, m)) = 2m + nm$ for $n, m \geq 2$.

Now, we will characterize the non-existence of lea $(a, d)$ coloring of $amal(K_1+G_n, K_1, m)$, for any grah $G$ of order $n$. We present it in the following theorem.

**Theorem 4.** *For $n, m \geq 2$, the lea$(a, d)$ coloring of graph $amal(K_1 + G_n, K_1, m)$ does not exist for $d \in \{0, 2\}$.*

*Proof.* The graph $amal(K_1 + G_n, K_1, m)$ is a connected and simple graph with vertex set $V(amal(K_1 + G_n, K_1, m)) = \{x\} \cup \{x_{i,j}; 1 \leq i \leq n, 1 \leq j \leq m\}$ and edge set $E(amal(K_1 + G_n, K_1, m)) = \{xx_{i,j}; 1 \leq i \leq n, 1 \leq j \leq m\} \cup \{x_{j,k}x_{j,l}; 1 \leq j \leq m, \{k, l\} \in V(G_n)\}$. Thus $|V(amal(K_1 + G_n, K_1, m))| = |V(G_n)|m + 1 = nm + 1$ and $|E(amal(K_1 + G_n, K_1, m)| = nm + m|E(G)|$. Based on Observation 6, we have $d \leq \frac{2p-4}{k-1} \longleftrightarrow d \leq \frac{2|V(amal(K_1+G_n,K_1,m))|-4}{|V(amal(K_1+G_n,K_1,m))|-2} \longleftrightarrow d \leq 2$.

Now, we will show the non-existence of lea$(a, d)$ coloring of $amal(K_1 + G_n, K_1, m)$ by defining $f : V(amal(K_1 + G_n, K_1, m)) \to \{1, 2, 3, \ldots, |V(amal(K_1 + G_n, K_1,$ $m))|\}$ as vertex labels of $amal(K_1 + G_n, K_1, m)$. First, for the non-existence $(a, 0)$-edge antimagic coloring. Assume that we have $d = 0$. For any $\{x_{i,j}, x_{i,k}\} \in V(amal(K_1 +$ $G_n, K_1, m))$ and $1 \leq i \leq n, 1 \leq j, k \leq m$, we will have $w(xx_{i,j}) = w(xx_{i,k})$. It contradicts with the definition of local antimagic coloring, since $xx_{i,j}$ and $xx_{i,k}$ are incident, they should have distinct edge weight as the colors. Thus $(a, 0)$-edge antimagic coloring of $amal(K_1 + G_n, K_1, m)$ does not exist.

Furthermore, we will prove the non-existence of local $(a, 2)$-edge antimagic coloring of $amal(K_1+G_n, K_1, m)$. Since, we have $f : V(amal(K_1+G_n, K_1, m)) \to \{1, 2, 3, \ldots, |V(amal$ $(K_1 + G_n, K_1, m)|\}$ as vertex labels of $amal(K_1 + G_n, K_1, m)$. We have three possible labels of the label of $f(x)$. First $f(x) = 1$, otherwise $f : V(amal(K_1 + G_n, K_1, m)\backslash\{x\} \to$ $\{2, 3, \ldots, |V(amal(K_1 + G_n, K_1, m)|\}$. The edge weight will be $W(xx_{i,j}) = \{3, 4, 5, \ldots, |V$ $(amal(K_1 + G_n, K_1, m))| + 1\}$. This form an arithmetic sequence of $d = 1$, since all $x_{ij}$ connects to $x$. It proves the non-existence of $d = 2$. The second possibility is to assign the vertex labels with $2 \leq f(x) \leq |V(amal(K_1 + G_n, K_1, m))| - 1$. Given that $s \in \{2, 3, \cdots, |V(amal(K_1 + G_n, K_1, m))| - 1\}$, choose any $s$ for $f(x) = s$. The edge weight will be $W(xx_{i,j}) = \{\cdots, 2s-3, 2s-2, 2s-1, 2s+1, 2s+2, 2s+3, \cdots\}$. This edge weight does not form an arithmetic sequence of different $d$, since even the different of the left and the right terms shows $d = 1$, but the middle terms $2s+1-(2s-1) = 2$. It shows that for any $f(x) = s$ where $s \in \{2, 3, \cdots, |V(amal(K_1+G_n, K_1, m))|-1\}$, the local $(a, 2)$-edge antimagic coloring of $amal(K_1 + G_n, K_1, m)$ does not exist. The third, assume that $f(x) = |V(amal(K_1 + G_n, K_1, m))|$, the edge weight will be $W(xx_{i,j}) = \{|V(amal(K_1 +$ $G_n, K_1, m))| + 1, |V(amal(K_1 + G_n, K_1, m))| + 2, \cdots, 2|V(amal(K_1 + G_n, K_1, m))| - 1\}$. This form an arithmetic sequence of $d = 1$, since all $x_{ij}$ connects to $x$. It proves the non-existence of $d = 2$. Thus $(a, 2)$-edge antimagic coloring of $amal(K_1 + G_n, K_1, m)$ does not exist. It concludes the proof.

## 3.2. Modeling Temporal-Spatial Dependencies with Graph-Based Deep Learning

In this work, we propose a Spatio-Temporal Graph Neural Network (STGNN) architecture tailored to forecast multivariate time series data derived from structured spatial observations such as nutrient content (e.g., nitrogen, phosphorus, potassium). The model is designed to jointly capture spatial dependencies across graph-structured nodes and temporal dynamics across multiple time steps, as illustrated in Figure 1 and detailed in Table 1.

The input feature matrix consists of sequential observations mapped onto a spatial graph, where each node represents a measurement location and edges encode spatial adjacency or correlation. The preprocessing layer performs normalization and an initial fully connected transformation to enhance feature richness. These features are then passed into a graph convolutional layer, which extracts spatial relationships via topological filtering using Graph Convolutional Networks (GCNs).

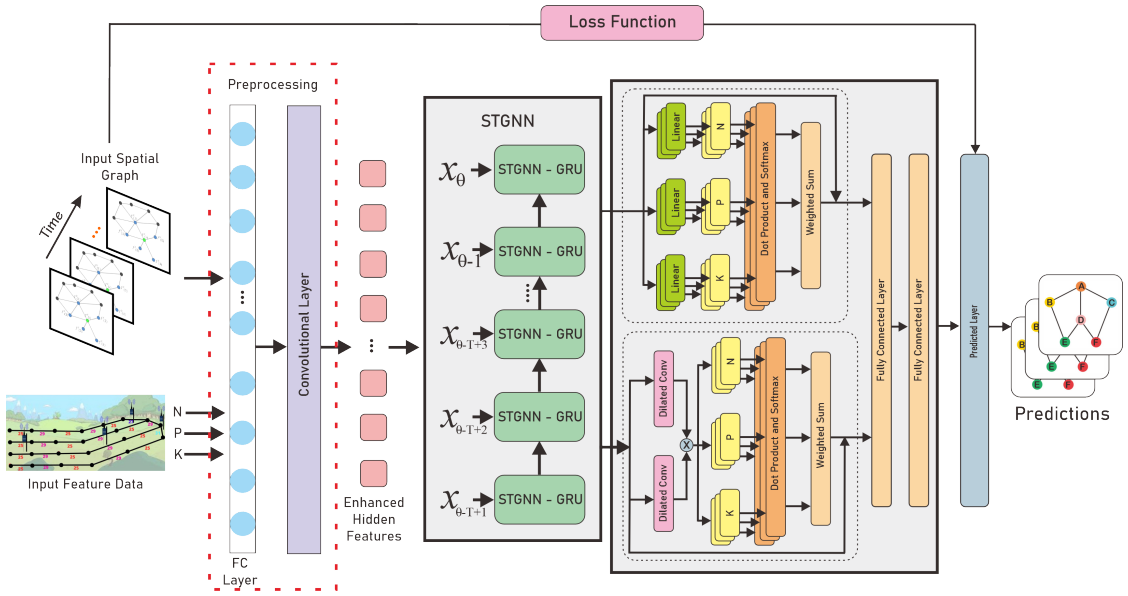


Figure 1: STGNN Model Architecture Visualization.

For temporal modeling, the architecture stacks a series of STGNN blocks, each combining spatial representations with Gated Recurrent Unit (GRU)-based processing to capture sequential dependencies. Each temporal slice of the enhanced hidden features is individually passed through an STGNN-GRU unit, enabling the model to learn both short-term and long-term trends. An attention mechanism further refines the temporal features by weighting them based on relevance to the forecasting task.

The aggregated output is then passed through multiple fully connected layers to project the learned embeddings into the prediction space. The final prediction layer outputs three continuous values per node, corresponding to target variables (e.g., discharge, depth, and width). The model is trained using the Adam optimizer for 200 epochs, with a learning rate of 0.01, and optimized using Mean Squared Error (MSE) loss. The use of optional components such as dilated convolution enhances the temporal receptive field, while regularization strategies (e.g., dropout) can be applied for improved generalization. Overall, the architecture demonstrates strong performance in learning spatial-temporal patterns from graph-structured data.

## 3.3. Spatio-Temporal Graph Encoding for Nutrient Forecasting

The next research result is the implementation of the $\chi_{le(a,d)}$ coloring scheme on precision agriculture. From now on, we will do time series forecasting on precision agriculture soil nutrient dataset, namely nitrogen, phosporus, and potassium. The dataset is obtained from the simulation of placing the capacitive sensor for soil nutrients. The placement of those sensors respects to the planting topology derived from Theorem 1, and the number of soil nutrient sensors is equalto the obtained lea$(a, d)$ chromatic number $\chi_{le(a,d)}(G)$.

The soil nutrient dataset that we obtained is subsequently used as the input for training

Table 1: Architectural Components and Parameters of the Proposed STGNN Model

| No. | Component | Description |
|---|---|---|
| 1 | Input Spatial Graph | Represents spatial structure over time. Nodes correspond to measurement units; edges reflect proximity or correlations. |
| 3 | Preprocessing Layer | Applies normalization and temporal alignment. Initial fully connected (FC) transformation to increase feature richness. |
| 4 | Convolutional Layer | Applies GCN operation over the input spatial graph to learn spatial dependencies from graph topology. |
| 5 | STGNN Block (Temporal Stack) | Sequence of STGNN-GRU units processing temporal slices of graph-encoded data (e.g., $X_{\theta-T+3}$ to $X_\theta$). Captures temporal dynamics. |
| 6 | Attention Mechanism | Includes dense projections and softmax weighting to emphasize relevant temporal features. Dot product used to compute weighted representation. |
| 7 | Dilated Convolution (Optional) | Extracts multi-scale temporal features through dilated convolutions across time-delayed embeddings. Enhances long-range dependencies. |
| 8 | Fully Connected Layers | Maps temporal-spatial feature embeddings to prediction space via dense layers. Usually two stacked layers. |
| 9 | Prediction Layer | Outputs 3-dimensional predictions (e.g., Nitrogen (N), Phosporus (P), and Potassium (K) per node per time step. |

the STGNN model. We analyze the NPK nutrient fertilization levels of plants across twenty-three plantations. First, we perform the vertex embedding process using a single-layer STGNN applied to a graph with three feature variables observed over 37 consecutive days. In total, the dataset consists of $23 \times 3 \times 37 = 2{,}553$ entries, corresponding to 23 plantation nodes, 3 soil nutrient features, and 37 time steps.

In accordance with the algorithm described previously, we conduct node embedding across all twenty-three plantation nodes. This embedding process transforms the original three-dimensional feature vector into a one-dimensional representation using message passing and aggregation techniques. During the message passing stage, each node is assumed to contain relevant information, which is transmitted to its neighboring nodes to support the learning process.

Thus, in this process, we consider the adjacency matrix with self-loops included. Instead of using the standard adjacency matrix $P$, we modify it by adding an identity matrix,

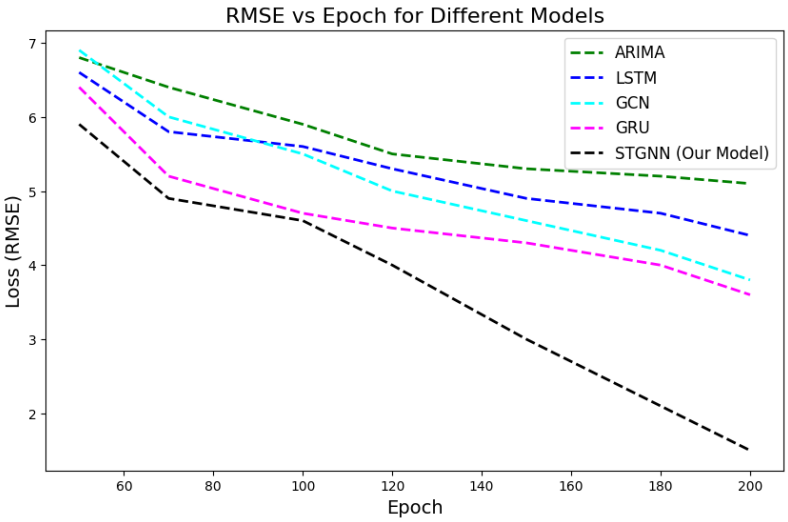


Figure 2: Visualization of the performance of the STGNN model and other models.

resulting in $Q = P + I$. Following the steps outlined in the algorithm above, we obtain time series data that are ready for analysis using the STGNN framework.

To evaluate the effectiveness of the node embeddings, we assess the proximity of nodes in both the original network and the embedding space. The embedding error is computed by comparing each pair of adjacent nodes using the infinity norm. Subsequently, we extend the model to perform multi-step time series forecasting with STGNN, using 60% of the data for training. The model's performance is evaluated by measuring the Root Mean Square Error (RMSE) or Mean Square Error (MSE) on the testing data. The results are presented in Figure 2.

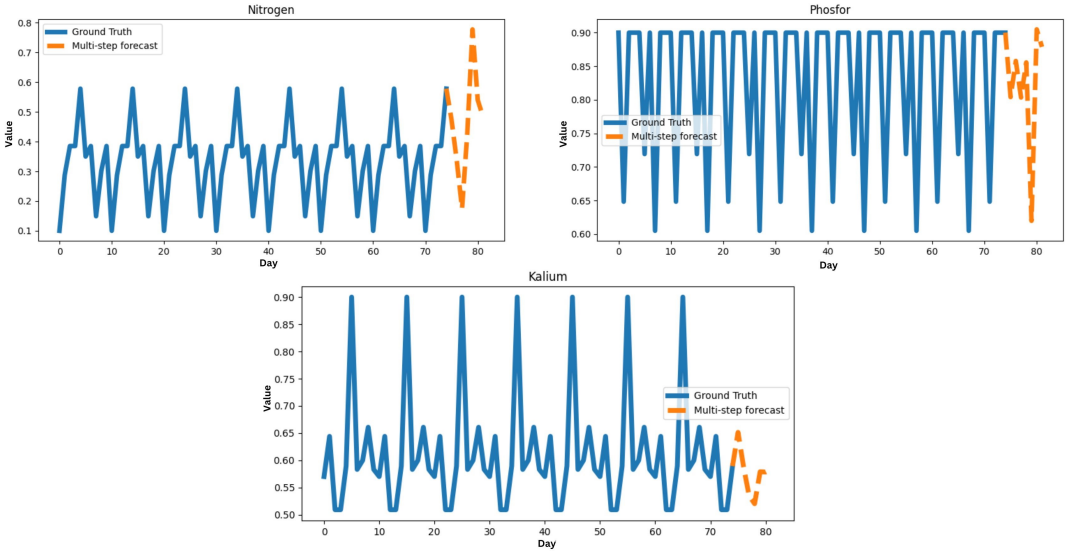


Figure 3: Forecast results using STGNN.

To evaluate the robustness and predictive capability of the proposed STGNN model, we conducted a comprehensive comparison with five baseline models: Historical Average (HA), Auto-Regressive Integrated Moving Average (ARIMA), Support Vector Regression (SVR), Graph Convolutional Network (GCN), and Gated Recurrent Unit (GRU). The comparative performance across models is illustrated in Figure 2, Figure 3, and summarized in Table 2.

As shown in Figure 2, the STGNN model consistently achieves lower RMSE values compared to the other methods over 200 epochs. The convergence curve of STGNN demonstrates a smooth and steady decrease in loss, indicating its stability and efficiency in the training process. Unlike GRU and GCN models which exhibit oscillations in early epochs, STGNN achieves optimal convergence with minimal variance, highlighting its robustness in handling temporal dependencies and spatial structures.

Table 2: The prediction results of the STGNN model and other baseline methods.

| Epochs | Metric | Model | | | | |
|---|---|---|---|---|---|---|
| | | ARIMA | LSTM | GCN | GRU | STGNN (Our Model) |
| 50 | RMSE | 8.1051 | 7.5357 | 9.2706 | 4.0482 | 3.9052 |
| | MAE | 6.1092 | 4.9198 | 7.2665 | 2.6803 | 2.6061 |
| | Accuracy | 0.3178 | 0.6871 | 0.6422 | 0.7068 | 0.7206 |
| | $R^2$ | 0.0732 | 0.8101 | 0.6037 | 0.8437 | 0.8531 |
| 100 | RMSE | 8.2112 | 7.4736 | 9.3430 | 4.0768 | 3.9606 |
| | MAE | 6.2143 | 4.9719 | 7.3101 | 2.7007 | 2.6441 |
| | Accuracy | 0.4271 | 0.6976 | 0.6305 | 0.7147 | 0.7165 |
| | $R^2$ | 0.0724 | 0.8131 | 0.6086 | 0.8367 | 0.8413 |
| 150 | RMSE | 8.2121 | 7.4753 | 9.4022 | 4.1002 | 3.9840 |
| | MAE | 6.2143 | 5.0321 | 7.3704 | 2.7107 | 2.6655 |
| | | 0.4260 | 0.6975 | 0.6373 | 0.7032 | 0.7142 |
| | $R^2$ | 0.0826 | 0.8131 | 0.6027 | 0.8350 | 0.8409 |
| 200 | RMSE | 8.2052 | 7.4872 | 9.4404 | 4.1131 | 4.0031 |
| | MAE | 6.2108 | 5.0604 | 7.4110 | 2.7321 | 2.6878 |
| | Accuracy | 0.4272 | 0.6971 | 0.6255 | 0.7015 | 0.7128 |
| | $R^2$ | 0.0814 | 0.8144 | 0.5888 | 0.8432 | 0.8703 |

Table 2 further confirms the superior performance of STGNN across multiple evaluation metrics, including RMSE, MAE, accuracy, and the coefficient of determination ($R^2$). At every evaluated epoch interval (50, 100, 150, and 200), STGNN achieves the lowest error values and the highest accuracy and $R^2$ scores, outperforming all baseline methods. Notably, the RMSE and MAE values of STGNN are significantly lower, while its $R^2$ values remain consistently above 0.85, demonstrating a strong fit between the predictions and the actual observations.

In addition, multi-step forecasting results, as presented in Figure 3, show the STGNN model's capability to accurately predict soil nutrient concentrations (nitrogen, phosphorus, and potassium) over a 20-day horizon. The predicted curves closely follow the ground truth

across all three nutrient types, reaffirming the model's generalization ability in real-world agricultural time series data.

Furthermore, to optimize the monitoring system in companion plantations, we applied the concept of local $(a, d)$-edge antimagic coloring to minimize the number of sensors required. Based on this approach, only four representative sensor locations are needed, corresponding to four plant types: Rosa sp., Bromeliaceae, Bougainvillea spectabilis, and Cryptanthus sp. These representative sensors, selected based on graph labeling theory, are sufficient to capture the overall dynamics of the plantation system, providing a cost-effective yet reliable monitoring strategy. Overall, the integration of STGNN with local graph-based optimization offers a promising framework for precision agriculture, enabling both accurate forecasting and efficient deployment of sensing resources.

## 3.4. Computational Complexity and Training Time Analysis

To evaluate the computational efficiency of the proposed STGNN model, we compared its training time to several baseline models, including ARIMA, LSTM, GCN, and GRU. Although STGNN integrates both graph convolutional layers and recurrent temporal processing, which intuitively may introduce additional computational cost, the model demonstrates efficient convergence behavior and outperforms the other models in terms of predictive accuracy, as discussed in earlier sections.

Table 3: Training Time Comparison of Models (200 Epochs)

| **Model** | **Training Time (seconds)** |
|---|---|
| ARIMA | 25.4 |
| LSTM | 102.8 |
| GCN | 94.6 |
| GRU | 86.3 |
| **STGNN (Our Model)** | **108.7** |

Figure 4 presents a visual comparison of the average training time required by each model over 200 epochs, while Table 3 provides the corresponding numerical values. As shown, STGNN required 108.7 seconds to complete 200 training epochs, which is slightly higher than GCN and GRU, but comparable to LSTM and still within a practical computational range. Notably, although ARIMA is the fastest with only 25.4 seconds, it performs poorly in terms of forecasting accuracy, as previously shown in Table 2.

This analysis highlights the trade-off between computational cost and prediction performance. While STGNN has a higher training time than simpler models, it offers substantial improvements in RMSE, MAE, and $R^2$ scores. Given its ability to learn spatial and temporal dependencies effectively, STGNN presents a balanced and scalable solution suitable for real-world agricultural forecasting applications, where both accuracy and robustness are crucial.

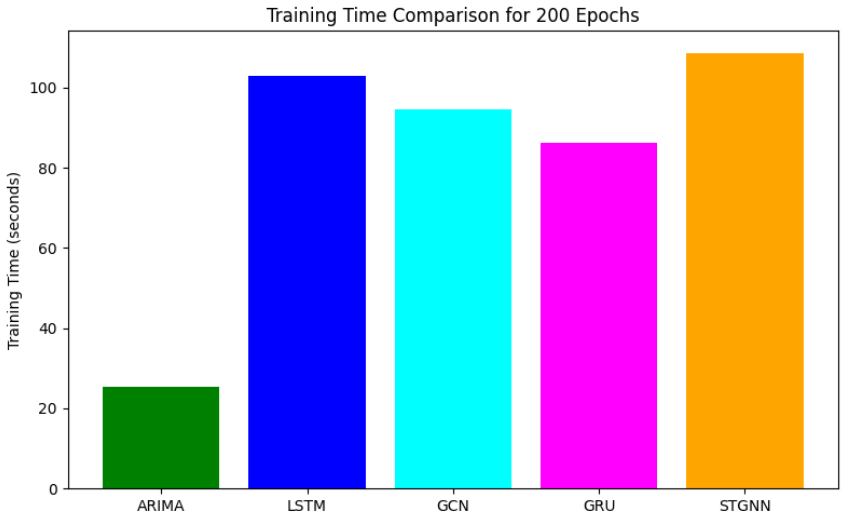


Figure 4: Training time comparison over 200 epochs for different models.

## 4. Concluding Remarks

This study introduced a hybrid framework that integrates local $(a, d)$-edge antimagic labeling and Spatio-Temporal Graph Neural Networks (STGNN) to forecast soil nutrient dynamics in companion plantations. The labeling technique was used to optimize sensor placement by identifying representative nodes, reducing the number of sensors from 23 to just four without compromising coverage. Meanwhile, the STGNN model effectively captured spatial and temporal dependencies, outperforming baseline models such as ARIMA, LSTM, GCN, and GRU across RMSE, MAE, accuracy, and $R^2$ metrics. The results confirmed that STGNN achieves high predictive performance and converges efficiently.

The integration of graph labeling and deep learning offers both theoretical and practical contributions. Theoretically, it extends the applicability of local antimagic labelings to data-driven graph learning. Practically, it provides a scalable solution for precision agriculture, enabling cost-efficient monitoring and accurate forecasting. Future work may explore dynamic graphs, enhance training efficiency, and adapt this approach to broader domains such as environmental monitoring and smart farming systems.

## Acknowledgements

This work was supported in part by LP2M-University of Jember and PUI-PT Combinatorics and Graph, CGANT-University of Jember, for their excellent collaboration and support in completing this study for the year 2025.

## References


[1] I. H. Agustin, M. Hasan, Dafik, R. Alfarisi, and R. M. Prihandini. Local edge antimagic coloring of graphs. *Far East Journal of Mathematical Sciences (FJMS)*, 102(9):1925–1941, 2017.

[2] I. H. Agustin, M. Hasan, Dafik, R. Alfarisi, A. I. Kristiana, and R. M. Prihandini. Local edge antimagic coloring of comb product of graphs. In *Journal of Physics: Conference Series*, 2018.

[3] S. Aisyah, R. Alfarisi, R. M. Prihandini, A. I. Kristiana, and R. Dwi. On the local edge antimagic coloring of corona product of path and cycle. *CAUCHY – Jurnal Matematika Murni dan Aplikasi*, 6(1):40–48, 2019.

[4] Z. L. Al Jabbar, Dafik, R. Adawiyah, E. R. AlbIrri, and I. H. Agustin. On rainbow antimagic coloring of some special graphs. In *Journal of Physics: Conference Series ICOPAMBS 2019*, pages 1465, 1–8, 2020.

[5] I. H. Agustin, Dafik, E. Y. Kurniawati, Marsidi, N. Mohanapriya, and A. I. Kristiana. On the local $(a, d)$-antimagic coloring of graphs. 2022.

[6] Dafik, I. L. Mursyidah, I. H. Agustin, R. I. Baihaki, F. G. Febrinanto, S. Husain, S. K. Binti, and R. Sunder. On rainbow vertex antimagic coloring and its application on stgnn time series forecasting on subsidized diesel consumption. *IAENG International Journal of Applied Mathematics*, 54(5), 2024.

[7] A. I. Kristiana, E. Rachmasari, I. H. Agustin, I. L. Mursyidah, and R. Alfarisi. On b-coloring analysis of graphs: An application to spatio-temporal graph neural networks for multi-step time series forecasting of soil moisture and ph in companion farming. *European Journal of Pure and Applied Mathematics*, 17(4):3356–3369, 2024.

[8] R. Alfarisi, R. M. Prihandini, R. Adawiyah, E. R. AlbIrri, and I. H. Agustin. Graceful chromatic number of unicyclic graphs. In *Journal of Physics: Conference Series*, volume 1306, page 012039. IOP Publishing, 2019.

[9] Dafik, I. H. Agustin, Surahmat, R. Alfarisi, and S. Sy. On non-isolated resolving number of special graphs and their operations. *Far East Journal of Mathematical Sciences*, 102(10):2473–2492, 2017.

[10] B. J. Septory, M. I. Utoyo, B. Sulistiyono, and I. H. Agustin. On rainbow antimagic coloring of special graphs. In *Journal of Physics: Conference Series*, volume 1836, page 012106. IOP Publishing, 2021.

[11] A. W. Gembong and I. H. Agustin. Bound of distance domination number of graph and edge comb product graph. In *Journal of Physics: Conference Series*, volume 855, page 012014. IOP Publishing, 2017.

[12] R. Sundaramoorthy and N. M. Chettiar. On $(a, d)$-edge local antimagic coloring number of graphs. *Turkish Journal of Mathematics*, 46:1994–2002, 2022.

[13] I. H. Agustin, Dafik, E. Y. Kurniawati, M. Marsidi, N. Mohanapriya, and A. I. Kristiana. On the local edge $(a, d)$-antimagic coloring of graphs: A new notion. In *5th International Conference on Current Scenario in Pure and Applied Mathematics (ICCSPAM-2022)*, volume 2718, page 020002. AIP Publishing LLC, 2023.

[14] F. P. Almaidah, Dafik, A. I. Kristiana, R. Adawiyah, R. M. Prihandini, and I. H.

Agustin. On local $(a, d)$-antimagic coloring of some specific classes of graphs. In *ICCGANT 2022*, pages 156–169, 2023.

[15] E. D. Putra, Dafik, A. I. Kristiana, R. Adawiyah, and R. M. Prihandini. On local $(a, d)$-edge antimagic coloring of some specific classes of graphs. In *ICCGANT 2022*, pages 42–53, 2023.

[16] R. Izza, Dafik, and A. I. Kristiana. On local $(a, d)$-edge antimagic coloring. In *Proceedings of the 6th International Conference of Combinatorics, Graph Theory, and Network Topology (ICCGANT)*, pages 30–41, 2023.

[17] A. I. Kristiana, E. Rachmasari, I. H. Agustin, I. L. Mursyidah, and R. Alfarisi. On b-coloring analysis of graphs: An application to spatial-temporal graph neural networks for multi-step time series forecasting of soil moisture and ph in companion farming. *European Journal of Pure and Applied Mathematics*, 17(4):3356–3369, 2024.

[18] S. N. N. Aziz, Dafik, I. M. Tirta, A. I. Kristiana, and E. Y. Kurniawati. On b-coloring analysis and its application on stgnn for soil moisture, temperature and ph forecasting of companion farming. In *AIP Conference Proceedings*, volume 3176, page 030031. AIP Publishing LLC, 2024.

[19] D. Mufidati, Z. R. Ridlo, I. N. Maylisa, and Dafik. Time series forecasting analysis of soil moisture by using artificial neural networks based-on rainbow antimagic coloring for autonomous irrigation system on horizontal farming. In *1st International Conference on Neural Networks and Machine Learning 2022 (ICONNSMAL 2022)*, pages 234–256. Atlantis Press, 2023.

[20] R. Sunder, I. H. Agustin, Dafik, I. N. Maylisa, N. Mohanapriya, and M. Marsidi. On local antimagic b-coloring and its application for stgnn time series forecasting on horizontal farming. *CAUCHY: Jurnal Matematika Murni dan Aplikasinya*, 10(1):117–132, 2025.